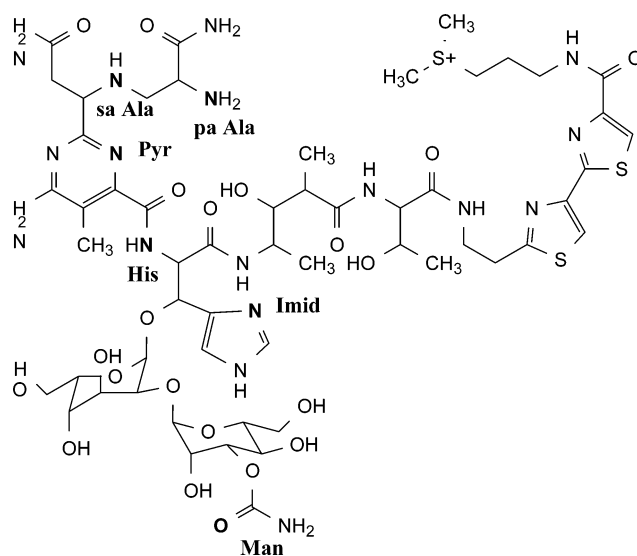


## Axial Ligation of Fe(II)–Bleomycin Probed by XANES Spectroscopy

Grigory Smolentsev,<sup>†</sup> Alexander V. Soldatov,<sup>\*,†</sup> Erik C. Wasinger,<sup>‡</sup> and Edward I. Solomon<sup>‡</sup>*Department of Physics, Rostov State University, Rostov-on-Don, 344090 Russia, and Department of Chemistry, Stanford University, Stanford, California 94305*

Received September 6, 2003

Full multiple scattering calculations of the Fe K-edge X-ray absorption near edge structure of bleomycin have been performed. Structural insight is based on the comparison between experimental and theoretical data calculated for different active site models coming from NMR-informed molecular dynamic simulations. In all models considered, the equatorial ligands (secondary amine in  $\beta$ -aminoalanine, pyrimidine and imidazole rings and the  $\beta$ -hydroxyhistidine) were left unchanged. Seven models with two axial ligands (the primary amine in  $\beta$ -aminoalanine and the carbonyl group of the mannose or a solvent molecule) were tested. The best agreement between theoretical and experimental spectra is achieved for the model of bleomycin with the primary amine and the oxygen of the mannose sugar occupying the axial positions. The coordination environment is characterized by serious distortions of the Fe octahedron, including the presence of one ligand with a very short bond length and significant angular distortions.



**Figure 1.** Structure of bleomycin. Fe ligands are marked in bold and labeled. Ligand abbreviations are the following: sa Ala, secondary amine of  $\beta$ -aminoalanine; Pyr, pyrimidine; Imid, imidazole ring; His, amine nitrogen of  $\beta$ -hydroxyhistidine; pa Ala, primary amine of  $\beta$ -aminoalanine; and Man, mannose.

Bleomycins (Blm) (see Figure 1) are a group of mononuclear glycopeptide-derived antibiotics that are used clinically as an anticancer therapy for neck, head, and testicular cancer and certain lymphomas.<sup>1</sup> The therapeutic effect of the drug is believed to arise from its ability to degrade DNA with sequence specificity.<sup>2</sup> Bleomycins bind a number of transition metal ions including Co, Fe, Cu, and Mn, but the highest activity is found when iron is bound to the drug. No crystal structure for ferrous bleomycin is known. Current insight into the metal arrangement and the overall structure of the complex is based on molecular dynamics, nuclear magnetic resonance, and spectroscopic results as well as on comparison with other forms of the antibiotic and related complexes.

The consensus structural data derived from these investigations are the following: the secondary amine in aminoalanine (sa Ala), the amide nitrogen in hydroxyhistidine (His), the N5 nitrogen in pyrimidine (Pyr), and the N1

nitrogen in imidazole ring (Imid) form the equatorial plane. The axial ligation of the Fe ion remains somewhat ambiguous, however. The initial metal coordination description was based on correlation with a biosynthetic precursor of Blm, Cu(II)P-3A,<sup>3</sup> which is missing both the bithiazole tail and sugar residue. Using X-ray diffraction, it was shown<sup>3</sup> that in addition to the above four equatorial ligands only the primary amine of Ala (pa Ala) coordinates to the Cu. All subsequent studies of this complex also favor this model.<sup>4–6</sup>

A combined methodology, which includes circular dichroism and magnetic circular dichroism in the near-infrared region, and pre-edge and EXAFS X-ray spectroscopy, was applied<sup>7</sup> to characterize the active metal arrangement in bleomycin and the model compound Fe–PMAH (macrocy-

\* To whom correspondence should be addressed. E-mail: Soldatov@rsu.ru.

<sup>†</sup> Rostov State University.

<sup>‡</sup> Stanford University.

(1) Lazo, J. S.; Sebt, S. M.; Schellens, J. H. *Cancer Chemother. Biol. Response Motif.* **1996**, *16*, 47.

(2) Burger, R. M. *Chem. Rev.* **1987**, *87*, 1107.

(3) Iitaka, Y.; Nakamura, H.; Nakatani, T.; Muraoka, Y.; Fujii, A.; Takita, T.; Umezawa, H. *J. Antibiot.* **1978**, *31*, 1070.

(4) Brown, S. J.; Stephan, D. W.; Mascharak, P. K. *J. Am. Chem. Soc.* **1988**, *110*, 1996.

(5) Farinas, E.; Tan, J. D.; Baidya, N.; Mascharak, P. K. *J. Am. Chem. Soc.* **1993**, *115*, 2996.

(6) Tan, J. D.; Hudson, S. E.; Brown, S. J.; Olmstead, M. M.; Mascharak, P. K. *J. Am. Chem. Soc.* **1992**, *114*, 3841.

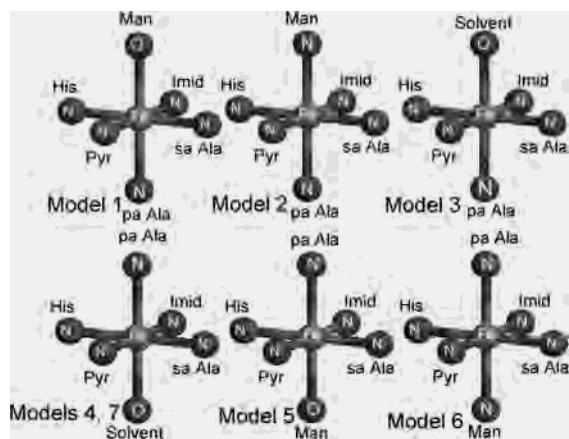


**Figure 2.** Schematic view of the 7 models from [11] used in the XANES simulations. Ligand abbreviations are the same as in Figure 1.

clic ligand with pyrimidine, imidazole, deprotonated amide, and secondary and primary amine functionalities). It was demonstrated that Fe–PMAH is five-coordinate in the solid state and six-coordinate in solution. Thus, the second axial position was assigned as the oxygen of a solvent molecule. For Fe(II)Blm, a six-coordinate state was also observed. However, from these results it is not possible to determine the nature of the second axial ligand for Blm. It can be nitrogen or oxygen of the carbonyl group of the mannose sugar (Man) or oxygen of the solvent water.

Very similar results were obtained using NMR<sup>8,9</sup> for Co(III)–OOH Blm. One axial ligand was assigned as the primary amine of Ala. The second axial position was occupied by an OOH group. An alternative model was proposed<sup>10</sup> for Peplomycin (Pep, related to Blm but with a modified bithiazole tail). In this model the primary amine of Ala is substituted by an OOH group while the second axial position is the carbonyl group of the mannose.

Recently, molecular dynamics (MD) simulations of Fe(II)–bleomycin with structure restrictions derived from NMR data were performed.<sup>11</sup> Seven models which represent different schemes of axial ligation were generated (see Figure 2). Comparison of the values of MD parameters and arguments based on correlations with bleomycin derivatives (such as Co(III)–OOH Blm) supported models 2 and 3. Analogous calculations for Co(II)Blm favored model 1.<sup>12</sup> The results summarized above indicate that there is no clear evidence supporting one model of axial ligation. There are three candidates for the second axial ligand: the nitrogen or oxygen of the mannose carbonyl group and the oxygen of a solvent molecule. In this paper, we present the first simulations of Fe K-edge XANES of Fe(II)Blm, which provide new insight into the Fe axial ligation.

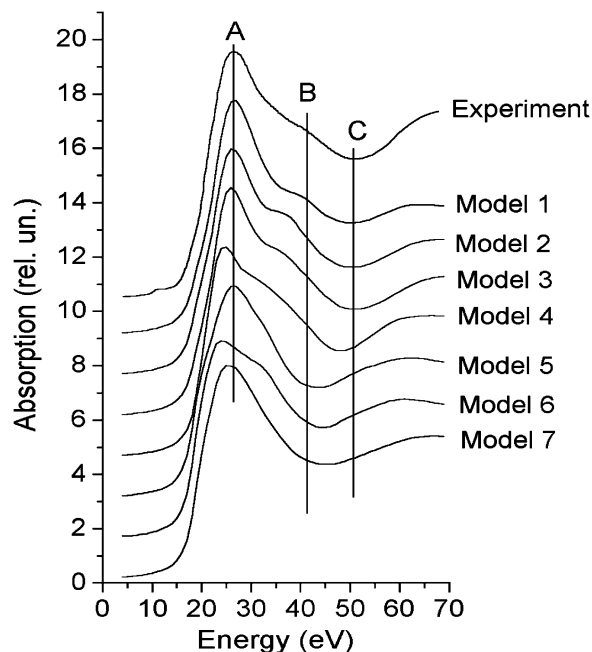


**Figure 3.** Experimental and theoretical Fe K-edge XANES of bleomycin. Calculations for 7 models in Figure 2<sup>11</sup> are shown.

The method of XANES calculations is based on a full multiple scattering scheme in the framework of the muffin-tin (MT) approximation. It has been described in detail elsewhere.<sup>13</sup> A cluster of 54 nearest to the Fe was chosen using the criterion of spectrum convergence as a function of cluster size. A molecular MT potential was obtained by a self-consistent-field scattering wave technique within the local density approximation. To take into account the broadening of the experimental spectrum according to the core hole lifetime, the finite mean free path of the photoelectron, and the experimental resolution, the calculated spectra were convoluted with a Lorentzian broadening function. We have used the value of 1.25 eV for the core hole bandwidth, an energy dependent function<sup>14</sup> representing all inelastic processes, and the value of 1.4 eV for the experimental resolution.

Calculations of the Fe K-edge XANES of bleomycin were performed for the 7 models generated using the MD technique,<sup>11</sup> schematically shown in Figure 2. All variants of axial ligation with the primary amine of Ala and different second ligands were tested. In model 4, the Fe ligation is the same as that in model 7, but the sugar moiety is close to the primary amine of Ala. Nevertheless, such reconstruction of the geometry leads to significant displacements of all Fe ligands, including equatorial plane groups. Moreover, the pa Ala group is very close to the equatorial plane in model 7. A more detailed description of the models has been given.<sup>11</sup>

Results of XANES simulations for all models and the experimental spectrum are presented in Figure 3. Experi-

(7) Loeb, K. E.; Zaleski, J. M.; Westre, T. E.; Guajardo, R. J.; Mascharak, P. K.; Hedman, B.; Hodgson, K. O.; Solomon, E. I. *J. Am. Chem. Soc.* **1995**, *117*, 4545.

(8) Xu, R. X.; Nettesheim, D.; Otvos, J. D.; Petering, D. H. *Biochemistry* **1994**, *33*, 907.

(9) Wu, W.; Vanderwall, D. E.; Lui, S. M.; Tang, X.-J.; Turner, C. J.; Kozarich, J. W.; Stubbe, J. *J. Am. Chem. Soc.* **1996**, *118*, 1268.

(10) Caceres-Cortes, J.; Sugiyama, H.; Ikudome, K.; Saito, I.; Wang, A. H.-J. *Eur. J. Biochem.* **1997**, *244*, 818.

(11) Lehmann, T. E. *J. Biol. Inorg. Chem.* **2002**, *7*, 305.

(12) Lehmann, T. E.; Serrano, M. L.; Que, L., Jr. *Biochemistry* **2000**, *39*, 3886.

(13) Della Longa, S.; Soldatov, A.; Pompa, A.; Bianconi, A. *Comput. Materials Science* **1995**, *4*, 199.

(14) Muller, J. E.; Jepsen, O.; Wilkins, J. W. *Solid State Commun.* **1982**, *42*, 365.

mental data were reported earlier.<sup>15</sup> As can be seen, the spectra split into two groups. Calculations for the models 1–4 correctly predict the relative energy separation between maximum A and minimum C, while this energy separation is very small for models 5–7. The shapes of spectra 1–3 between features A and C are very similar, but the position of shoulder B depends on the model. Thus, the energy position of feature B can be used as a criterion to choose the best local geometry. Spectra 2 and 3 have feature B shifted to lower energy than in the experimental data. Model 4 has a very broad and low energy shoulder while model 6 has a peak with too high intensity. Spectra 5 and 7 lack feature B. Thus, the best agreement between the experimental and theoretical spectra is achieved for model 1 with the mannose oxygen in the second axial position. This ligand configuration is consistent with variable-temperature variable-field magnetic circular dichroism studies<sup>16</sup> on derivatives of Fe(II)Blm. In Co(III)Blm, model 4 is favored from NMR studies.<sup>10</sup> However, this metal complex is in a different redox and spin state, and Co(III)Blm has an additional endogenous hydroperoxide bound to the metal ion.

One of the main questions in comparing spectra 1–3 is which changes in structural parameters can be correlated to differences in the XANES. To answer this question, we first calculated the spectrum for model 1, but with only the oxygen atom from the mannose residue coordinated to Fe. This structure is equivalent to model 3 in ligand connectivity, but with the atomic coordinates taken from model 1. Theoretical simulations for this cluster revealed very limited sensitivity of the spectrum to the presence of the outer shell atoms of the mannose. Next, substitution of this axial oxygen by a nitrogen atom (using the same coordinates in the first coordination shell) also leads to a weak reconstruction of the XANES.

Geometric distortion in the octahedron of atoms nearest to the Fe is a more realistic reason for the shift of peak B. Calculations with varied Fe–ligand bond lengths and ligand–Fe–ligand angles were performed. Bond length changes lead to an overall energy shift of the spectra and a slight change in the relative positions of maximum A and minimum C. Fitting of the spectrum using models 1–3 and varying average first shell distances result in a 0.03 Å bond length contraction. Alternatively, angular distortions lead to reconstruction of feature B. Thus, the key structural parameters that determine the position of shoulder B are ligand–Fe–ligand angles. Differences in this parameter for models 1–3 associated with the variation in the second axial ligand cause the shift of feature B. Nevertheless, the position of this shoulder was reproduced well using the angles in the models proposed by Lehmann. Therefore, the simulations were calculated with the angles fixed to those of the ref 11.

(15) Westre, T. E.; Loeb, K. E.; Zaleski, J. M.; Hedman, B.; Hodgson, K. O.; Solomon, E. I. *J. Am. Chem. Soc.* **1995**, *117*, 1309.

(16) Loeb, K. E.; Zaleski, J. M.; Hess, C. D.; Hecht, S. M.; Solomon, E. I. *J. Am. Chem. Soc.* **1998**, *120*, 1249.

**Table 1.** Ligand1–Fe–Ligand2 Bond Angles for Models 1–3 of Bleomycin As Derived from the NMR Study<sup>11</sup>

ligand1	ligand2	ligand1–Fe–ligand2 angle (deg)		
		model 1	model 2	model 3
pa Ala	Pyr	99	67	88
pa Ala	Imid	67	98	105
pa Ala	His	89	93	96
pa Ala	Sa Ala	67	79	79
Man/solvent	Pyr	86	97	95
Man/solvent	Imid	106	79	72
Man/solvent	His	84	91	93
Man/solvent	Sa Ala	121	99	93
Pyri	His	80	81	81
His	Imid	98	97	97
Imid	Sa Ala	103	105	104
sa Ala	Pyr	70	77	79

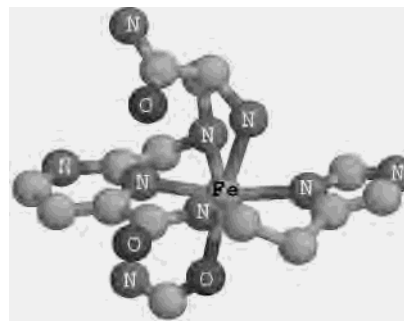


**Figure 4.** Pictorial view of the Fe arrangement for the model 1. Fe, N, and O atoms are marked. Other atoms are carbons.

Table 1 summarizes the ligand–Fe–ligand bond angles for models 1–3.<sup>11</sup> As one can see, pa-Ala–Fe–Imid, Man–Fe–Imid, and Man–Fe–sa-Ala bond angles for model 1 are very different for those in models 2 and 3. Substitution of one axial ligand does not seriously perturb the equatorial plane, but it deflects the other axial ligand (pa-Ala–Fe–Imid angle). Bond lengths obtained for model 1 correlate with recent EXAFS data.<sup>17</sup> It was shown for Fe(II)Pep, which has the same metal coordination environment as Blm, that there is a single ligand with a bond length of 1.87 Å and five ligands with an average Fe–ligand distance of 2.09 Å. For model 1, the atom closest to Fe is at a distance of 1.93 Å, and the five other atoms are located at an average of 2.09 Å.

In conclusion, we have shown that the model 1 (Figure 4)<sup>11</sup> of Fe(II)–Blm is the most realistic of the 7 considered perturbations. The key parameters that allow the use of XANES to distinguish this model from the other models with the same chirality are the angular distortions of the octahedron of nearest neighbor atoms coordinated to Fe.

**Acknowledgment.** We thank Prof. T. Lehmann (Instituto Venezolano de Investigaciones Científicas (IVIC), Venezuela) for sharing her structural data on Fe(II)–Blm and for useful discussions.

IC0350537

(17) Wasinger, E. C.; Zaleski, K. L.; Hedman, B.; Hodgson, K. O.; Solomon, E. I. *J. Biol. Inorg. Chem.* **2002**, *7*, 157.